Building Simulation 2009

Eleventh International IBPSA Conference
Glasgow, Scotland
July 27-30, 2009

NUMERICAL SIMULATION OF COLD AIR JET ATTACHMENT TO NON ADIABATIC WALLS

Nikola Mirkov[1], Žana Stevanović[1], and Žarko Stevanović[1]
Institute of Nuclear Sciences "Vinča", Laboratory for Thermal Engineering and Energy, Belgrade, Republic of Serbia

ABSTRACT

A jet of cold air is denser then ambient air but it adheres to the ceiling of the room over the given distance when it is blown horizontally close to it. Such behaviour of fluid jets is well-known as Coanda effect and it is widely used in practice like in the case of ventilation and air-conditioning of rooms. This phenomenon is not sufficiently known both in terms of mechanism and quantitative effects. The complexity is arising in the case of non-adiabatic ceiling that is common practice in real building structures, since the cold air jet, attachment distance is strongly influenced by heat flux thought the ceiling. The aim of this paper is to propose an algorithm of numerical simulation of fluid flow and heat transfer in the room and ceiling simultaneously, known as conjugate heat transfer problem. Using proposed model, uncertainty of heat transfer coefficient determination is avoided integrating the same general transport equation for fluid flow and heat transfer over the whole computational domain including both air movements in the room and ceiling solids.

INTRODUCTION

When a cold air jet is issued into quiescent surroundings bellow a ceiling parallel to the axis of the jet discharge, the so-called Coanda effect forces the jet to deflect towards the wall boundary and attach to the ceiling wall. After the jet impinges on the wall, the flow redevelops in the wall jet region.

This type of flow is often called wall attaching offset jet and it occurs in many engineering applications other then air-conditioning such as environmental discharges, heat exchangers, fluid injection systems, cooling of combustion chamber wall in a gas turbine and others.

From a computational perspective, airflows in the rooms are very complex. Due to this characteristics, they present a great challenge for the available numerical models.

Fig. 1 shows the scheme of room model where the regions of interest are depicted including diffuser exhaust and ceiling wall. Due to the entrainment of fluid between the jet and the upper wall, there is a reduction of pressure in this region forcing the jet to deflect towards the boundary and eventually attach with it. Along the attachment length fluid jet and solid wall thermally interact.

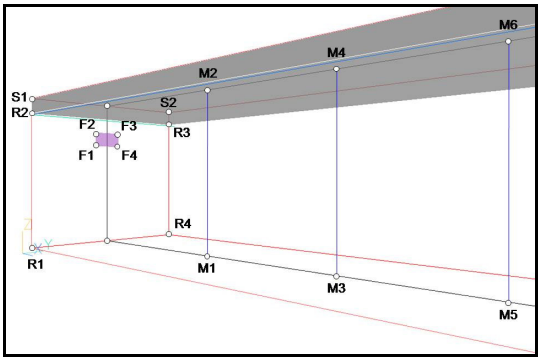

Figure 1 Scheme of Room Model

Legend:
R1-R2-R3-R4: First Cross-Section of Room (15m x 3m x 2.25m)
R2-S1-S2-R3: First Cross-Section of Wall (Ceiling: (15m x 3m x 0.25m))
F1-F2-F3-F4: Exhaust of Rectangular Diffuser (0.5m x 0.25m)
M1-M2: Central-Vertical Line on x/H=5
M2-M3: Central-Vertical Line on x/H=10
M2-M3: Central-Vertical Line on x/H=20

The present study is aimed at investigating the tri-dimensional turbulent fluid flow of wall attaching jet and conjugate heat transfer characteristics of fluid flow and solid wall.

A conjugate heat transfer problem occurs when the fluid regime is coupled with the conducting solid wall of finite thickness.

There have been numerous studies on wall jets, one study of cold air jet attachment to walls is presented in Marchal (1999). Kanna and Das (2005a) have studied the conjugate heat transfer of laminar plane wall jet and reported a closed-form solution for the interface temperature, local Nusselt number and average Nusselt number. The conjugate heat transfer of a laminar incompressible offset jet is reported in other paper by Kanna and Das (2005b). The ideas of conjugate heat transfer as they were presented here appear in Patankar (1980).

MATHEMATICAL MODEL

System of partial differential equations describing conservation of mass, mommentum and energy, together with two transport equations for turbulence kinetic energy and turbulence kinetic energy dissipation rate constituting Chen-Kim $k-\varepsilon$ turbulence model, has following form:

$$\frac{\partial \rho}{\partial t}+\frac{\partial}{\partial x_i}(\rho U_i)=0$$

$$\frac{\partial}{\partial t}(\rho U_i)+U_j\frac{\partial}{\partial x_j}(\rho U_i)-\frac{\partial}{\partial x_j}\left(\mu_{ef}\frac{\partial U_i}{\partial x_j}\right)=-\frac{\partial P}{\partial x_i}$$

$$\frac{\partial}{\partial t}(\rho T)+U_j\frac{\partial}{\partial x_j}(\rho T)-\frac{\partial}{\partial x_j}\left(\frac{\mu_{ef}}{Pr}\frac{\partial T}{\partial x_j}\right)=0 \qquad (1)$$

$$\frac{\partial}{\partial t}(\rho k)+U_j\frac{\partial}{\partial x_j}(\rho k)-\frac{\partial}{\partial x_k}\left\{\left(\mu+\frac{\mu_t}{\sigma_k}\right)\frac{\partial k}{\partial x_k}\right\}=$$
$$=\rho(G-\varepsilon)$$

$$\frac{\partial}{\partial t}(\rho \varepsilon)+U_j\frac{\partial}{\partial x_j}(\rho \varepsilon)-\frac{\partial}{\partial x_k}\left\{\left(\mu+\frac{\mu_t}{\sigma_\varepsilon}\right)\frac{\partial \varepsilon}{\partial x_k}\right\}=$$
$$=\rho\frac{\varepsilon}{k}\left(C_{\varepsilon 1}G-C_{\varepsilon 2}\varepsilon+C_{\varepsilon 3}G^2/k\right)$$

Which is uniquely defined with additional relations:

$$G=\nu_t\left(\frac{\partial U_i}{\partial x_k}+\frac{\partial U_k}{\partial x_i}\right)\frac{\partial U_i}{\partial x_k}$$

$$\mu_t=C_\mu\rho\frac{k^2}{\varepsilon} \qquad (2)$$

$$\mu_{ef}=\mu+\mu_t$$

$$\frac{P}{\rho}=RT$$

$$\sigma_k\,;\sigma_\varepsilon\,;\sigma_T\,;C_\mu\,;C_{\varepsilon 1}\,;\ C_{\varepsilon 2}\,;\ C_{\varepsilon 3}\ = 1.0;\ 1.314;$$
$$0.9;\ 1.44;\ 1.92;\ 0.25$$

Carefully looking at equations at this system we can observe that they have the same form of general equation of conservation of field, which was expected. Difference appears in additional terms on right hand side. If we generally name them source terms and denote with S_Φ, then we can alternatively write one represenative transport equation instead of writting system of equations (1). This equation will have the form:

$$\frac{\partial}{\partial t}(\rho\Phi)+U_j\frac{\partial}{\partial x_j}(\rho\Phi)-\frac{\partial}{\partial x_j}\left(\Gamma_\Phi\frac{\partial \Phi}{\partial x_j}\right)=S_\Phi \qquad (3)$$

First term on left hand side represents local change of variable Φ, then follows a convective term, and third term defines a diffusion of variable Φ. The form of general transport coefficient Γ_Φ depends on physical meaning of general variable Φ. This general form has significant adventage in defining numerical model because we need to define identical numerical algorithms for solving all partial differential equations of conservation.

Integrating system of partial differential equations (1) coupled with additional realtions (2), with defined initial and boundary conditions for each case separatly, we attain required solution field of physical parameters of fluid in defined space and time domain.

On the other hand this algorithm didn't solve the problem of heat transfer between fluid and solid wall, and problem of heat conduction in solid wall. Later problem is governed by well known equation of heat conduction in solids:

$$c_m\frac{\partial T_m}{\partial t}-\lambda_m\frac{\partial^2 T_m}{\partial x_j\partial x_j}=0 \qquad (4)$$

Where T_m stands for temperature of material, c_m and λ_m represent specific heat capacity and heat conduction coefficient of solid body respectively.

Classical approach in solving problem of heat transfer between fluid and solid wall is aplication of Newton's law of heat transfer.

$$q=\alpha\left(T_w-T_f\right) \qquad (5)$$

Where T_w is the solid wall temperature which is in contact with the fluid of temperature T_f, and α represents heat transfer coefficient. According to above relations it is clear that we need to know the value of the heat transfer coefficient and temperature distributions in order to determine the ammount of heat exchanged between the solid wall and the fluid.

Equation (5) has simple form but is very complex in the essence. Heat transfer coefficient is a function of several variables. In the first place it depends of thermophysical characteristics of fluid, velocity of fluid flow, flow character (laminar or turbulent) and heat exchange surface geometry. As a consequence of these characterictics coefficient of heat transer has attributes of local variable.

Previous theoretical and engineering practice of solving this problem have mostly been based on determing average coefficient of heat transfer - a process which leeds to reduction of solution accuracy. Most popular form of determing average coefficient of heat transfer is derived from criterial analysis trough Nusselt number:

$$Nu = \frac{\alpha L}{\lambda} \tag{6}$$

Where L represents characteristic scale of flow field. On the other side Nusselt number is a function of Prandtl and Reynolds number, in general form this function has following form:

$$Nu = a \cdot Pr^b Re^c \tag{7}$$

Where a, b, and c are empiricaly determined.
Shown classical way of solving this problem brings us to conclusion that even if the fields of physical parameters in flow field and solid wall are given in differential form, empirism in determing coefficient of heat transfer faces us with uncertanity of solution accuracy.
Quality of solution of partial differential equations of turbulent heat transfer and mommentum in fluid (1) and differential equations of heat conduction in solid wall (4) cannot be neglected, especially because equation (4) itself has the form of general transport equation (3). This is the main reason for searching alternative idea for the solution of given problem by discarding empirism connected with Newton's law.

Conjugate differential model of heat transfer in fluid and solid

The idea of conjugate differential model of heat transfer in fluid and solid lays in the possibility to treat the fluid and solid wall as a unique „flow space". In order to present this model in detail certain mathematical manipulations are executed on equation (4) so it is being recasted in the form of general transport equation and then added to the system of partial differential equations (1). Intergrating such system, empirical determination of heat transfer coefficient is avoided and the solution is obtained both for the fluid and solid wall domain.

Equation (4) can be rewritten in following form:

$$\frac{\partial}{\partial t}(\rho_m T_m) + 0 \cdot \frac{\partial}{\partial x_j}(\rho_m T_m) - \frac{\partial}{\partial x_j}\left(\frac{\rho_m \lambda_m}{c_m}\frac{\partial T_m}{\partial x_j}\right) = 0 \tag{8}$$

Where it can be written that $\Gamma_m = \rho_m \lambda_m / c_m$. Second, convective term is written intentionaly although it doesn't exist bacause we are dealing with solid domain. Therefore, if we somehow manage to define that part of flow space as belonging to solid, set velocity field equal to zero, and if we translate transport coefficient Γ_m and material density ρ_m to coresponding equivalent which holds for fluid, obatined differential equation will be valid for fluid space, and we have means to add it to system of partial differential equations (1). Equation (8) will undergo mathematical transformations. First it will be multiplied by ρ / ρ_m getting:

$$\frac{\partial}{\partial t}(\rho T_m) - \frac{\partial}{\partial x_j}\left(\frac{\rho \lambda_m}{c_m}\frac{\partial T_m}{\partial x_j}\right) = 0 \tag{9}$$

And then adjusting transport coefficient we get:

$$\frac{\partial}{\partial t}(\rho T_m) - \frac{\partial}{\partial x_j}\left(\frac{\rho \lambda_m}{c_m} \cdot \frac{c_P}{c_P} \cdot \frac{\lambda}{\lambda}\frac{\partial T_m}{\partial x_j}\right) = 0 \tag{10}$$

Knowing that relation for the transport coefficient in fluid is expressed by $\Gamma_{T_m} = \rho\lambda / c_P$, equation (10) becomes:

$$\frac{\partial}{\partial t}(\rho T_m) - \frac{\partial}{\partial x_j}\left(\frac{\lambda_m c_P}{\lambda c_m}\Gamma_{T_m}\frac{\partial T_m}{\partial x_j}\right) = 0 \tag{11}$$

Final step in obtaining differential equation of interest is introducing porosity of integational cell coefficient.

$$\beta_V = \frac{\lambda_m c_P}{\lambda c_m} \tag{12}$$

Finally we can conclude the procedure of transforming equation (4) which now has the form of equation valid for fluid flow domain.

$$\frac{\partial}{\partial t}(\rho T_m) - \frac{\partial}{\partial x_j}\left(\Gamma_{T_m}\frac{\partial T_m}{\partial x_j}\right) = 0 \tag{13}$$

where $\Gamma_{T_m} = \beta_V \Gamma_T$.

Formally and essentially equation (13) represents energy equation of system (1), so the number of equations in system (1) remained the same. Integrating energy equation is simultanious for fluid and solid domain, while it is necesary to define following conditions in order to have succesful integration.

1. Set velocity field to zero in domain of flow space which belongs to solid wall.

2. Introduce new dependant variable – the porosity coefficient β_V and set it to one in fluid part of domain, and having value of $\lambda_m c_p / c_m \lambda$ flow space which belongs to solid wall.

NUMERICAL SETUP AND BOUNDARY CONDITIONS

In this study mathematical model has been solved numerically using PHOENICS software.
For that purpose physical domain is divided by 75 x 40 x 50 cells where *75 x* 40 x 10 cells cover the solid wall. The flow is resolved down to viscous sub-layer and logarithmic wall functions are used for the first row of the cells. Numerical grid at central *X-Z* plane is shown in Figure 2.

Three cases have been considered with difference in flow speed at diffuser exhaust. Velocities are equal to 1, 1.5, and 2 *m/s* respectively. Temperature of issuing jet is 15 ^oC in all three cases. It is important to stress that wall surface temperature is not a boundary condition, it is calculated from the inner region. For the other side of the wall it is assumed that there are no heat sources or sinks. Brick is specified as a wall material.

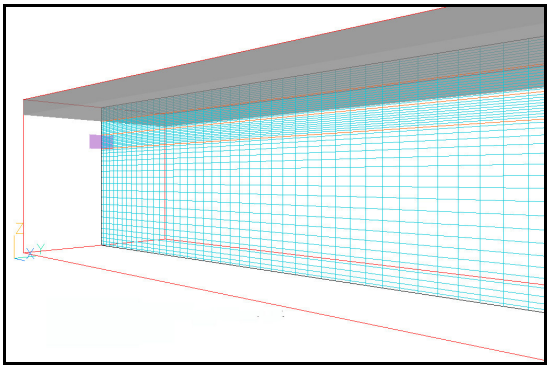

Figure 2 Numerical grid at central X-Z plane (75 x 40 x 50 = 150000 total number of cells, where 75 x 40 x 10 = 30000 cells cover the solid wall)

PRESENTATION OF RESULTS

Two sets or results are presented, first concerning flow field, where attaching the air jet to the ceiling due to Coanda effect becomes apparent, and second concerning temperature distribution in central vertical plane and in horizontal cross section of the wall placed five centimetres above the fluid-solid interface.

Horizontal component of velocity at central x-z plane for all three respective cases is shown in Fig. 3.

Temperature distribution in central vertical plane and in horizontal cross section of the wall placed five centimetres above the fluid-solid interface are shown in Figures 4, 5 and 6.

For the convenience of presenting the results in fluid flow, in order to comprise three-dimensional effect of flow, we chose to visualise the fictive surfaces with equal temperature (temperature iso-surface). Fig. 7, 8 and 9 show contours of the cold air jet by temperature iso-surfaces with value of 16 ^oC, just one degree above the temperature of air jet at diffuser exhaust.

Finally temperature distributions along central lines going trough both fluid and solid domain are shown on Fig. 10, Fig. 11. and Fig. 12 for each separate case respectively.

CONCLUSION

Our basic objective has been description of methodology for simultaneous computation of temperature distribution in room and surrounding walls. Principal idea and benefit of suggested procedure is elimination of uncertainty in determing coefficient of heat transfer and empirical relations connected to *Re* and *Nu* numbers. Practically, manipulating differential equation of thermal energy conservation and prescribing special boundary conditions in solid, model allows simultaneous integration of complete differential model in fluid and solid.

This paper doesn't have intention to verify quantitative results yet to present the methodology. As an adequate example, one that has certain complexion related with it, ceiling attaching wall jet exhibiting Coanda effect is simulated for different velocities of air flow.

Results shown in previous section are illustrative and clearly display good properties of suggested procedure.

One of the main disadvantages of the procedure is ability to be carried out only in case of differential model and corresponding numerical integration with available software of this class. In this paper we used FLAIR - special HVAC module of general code PHOENICS (www.cham.co.uk).

ACKNOWLEDGEMENT

This paper is concerned by the Project of Technical Development (No.TR-18004) funded by Serbian Government.

REFERENCES

Kanna P. R., Das M. K. 2005 (a). Conjugate forced convection heat transfer from a flat plate by laminar plane wall jet flow, International Journal of Heat and Mass Transfer 48 pp. 2896-2910.

Kanna P. R., Das M. K. 2005 (b). Conjugate heat transfer study of two-dimensional laminar incompressible offset jet flow. Numerical heart transfer: Part A. 48 (7) pp. 671-691.

Marchal D. 1999. L'adhérence des jets d'air froid au plafond des locaux climatises, International journal of Thermal Sciences, pp. 832-842

Patankar S. V. 1980. Numerical Heat Transfer and Fluid Flow. Hemisphere Publishing Corporation, Francis & Taylor Group, New York

NOMENCLATURE

G	Volumetric production rate of k
k	Turbulence kinetic energy
ε	Turbulence dissipation rate
Re	Reynolds number
Nu	Nusselt number
Γ_m	Transport coefficient
λ_m	Heat conduction coefficient
c_m	Specific heat capacity
T_f	Fluid temperature
T_w	Wall temperature
α	Teat transfer coefficient
β_V	Integrational cell porosity

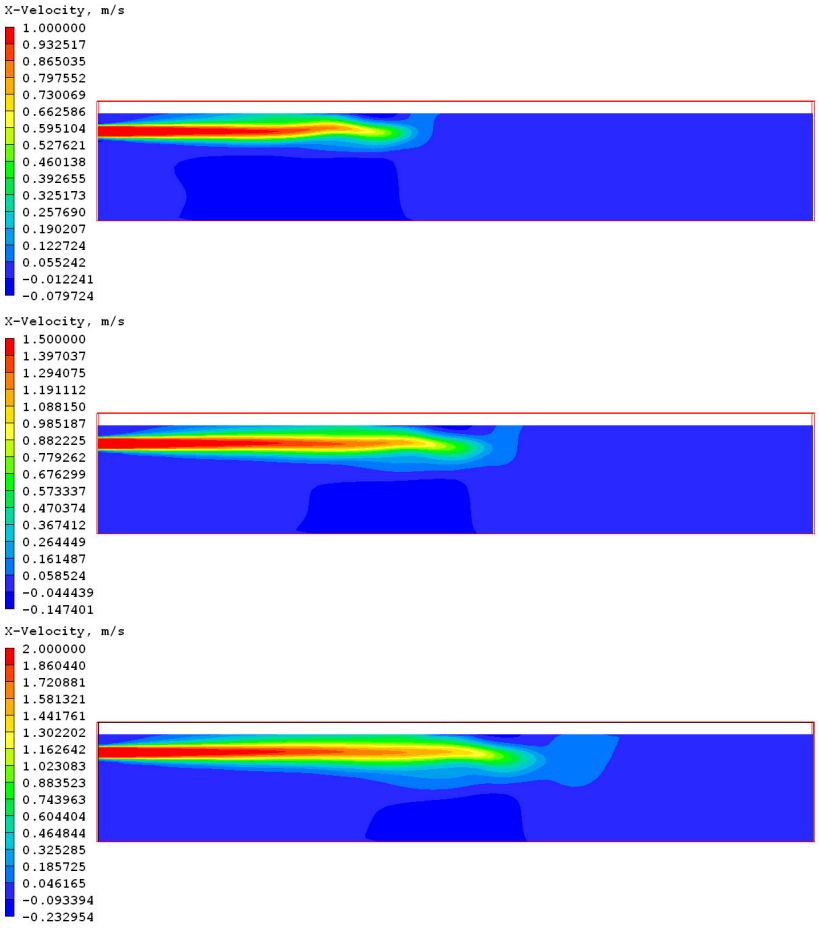

Figure 3 Air Flow Field: U-velocity at central x-z plane (Top: Case 1, inlet velocity equal to 1 m/s, Middle: Case 2, inlet velocity equal to 1.5 m/s, Bottom: Case 3, inlet velocity equal to 2 m/s)

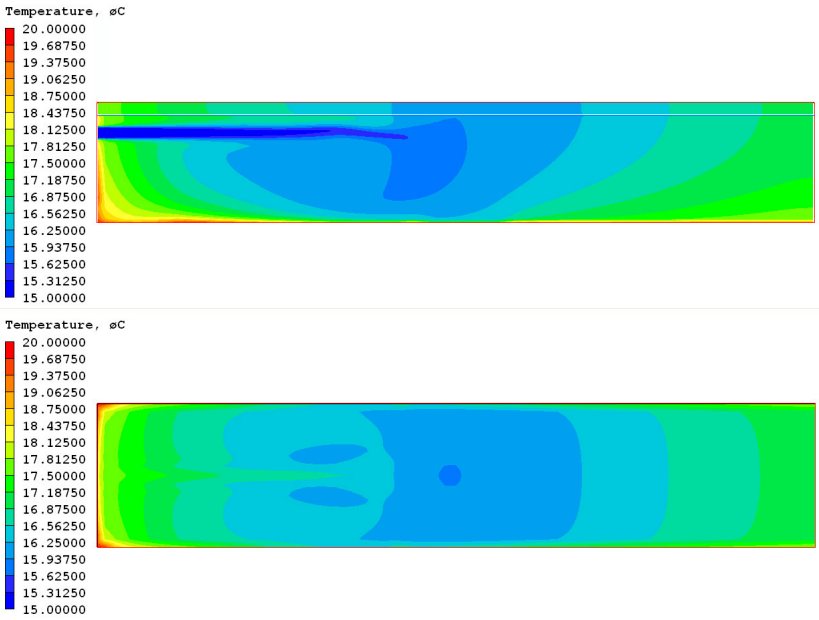

Figure 4 Temperature Field for Case 1 (Top: Central x-z plane; Bottom: solid x-y plane at z=2.3m)

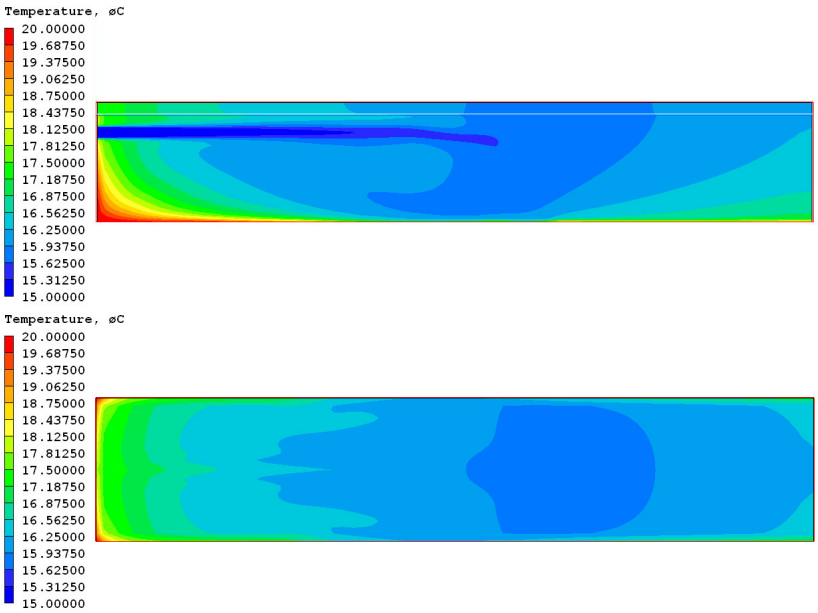

Figure 5 Temperature Field for Case 2 (Top: Central x-z plane; Bottom: solid x-y plane at z=2.3m)

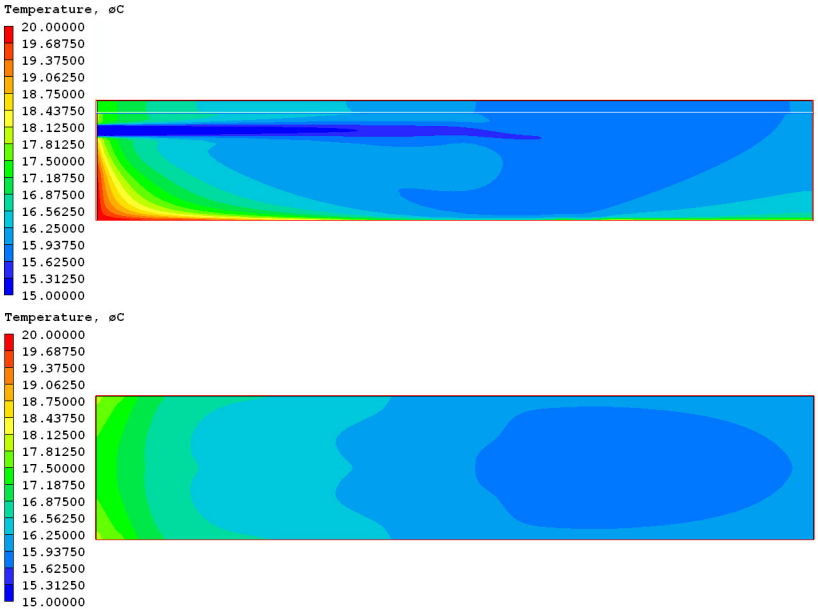

Figure 6 Temperature Field for Case 3 (Top: Central x-z plane; Bottom: solid x-y plane at z=2.3m)

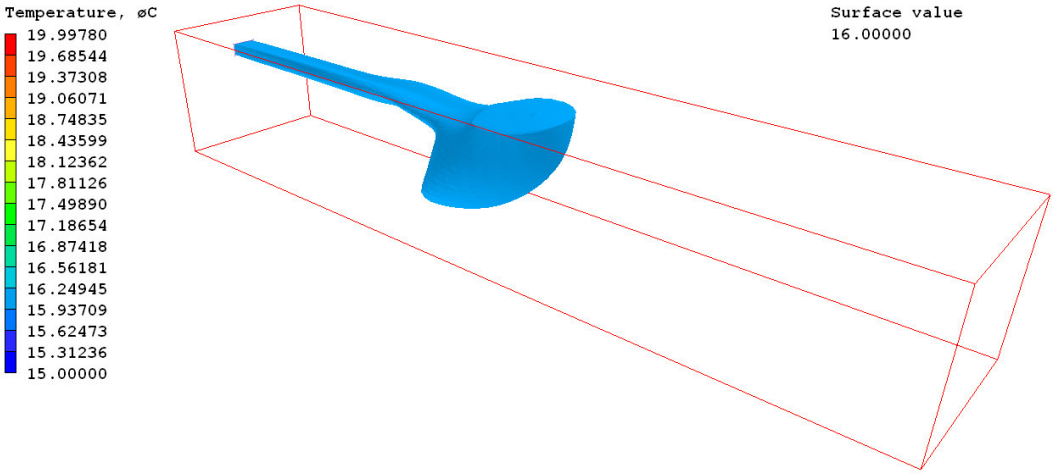

Figure 7 Temperature Iso-Surface of 16 ^{o}C for Case 1.

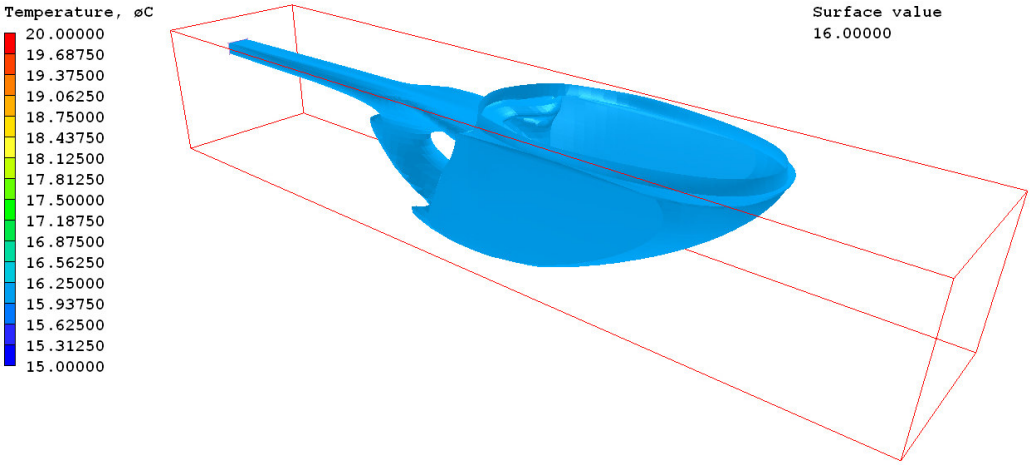

Figure 8 Temperature Iso-Surface of 16 ^{o}C for Case 2.

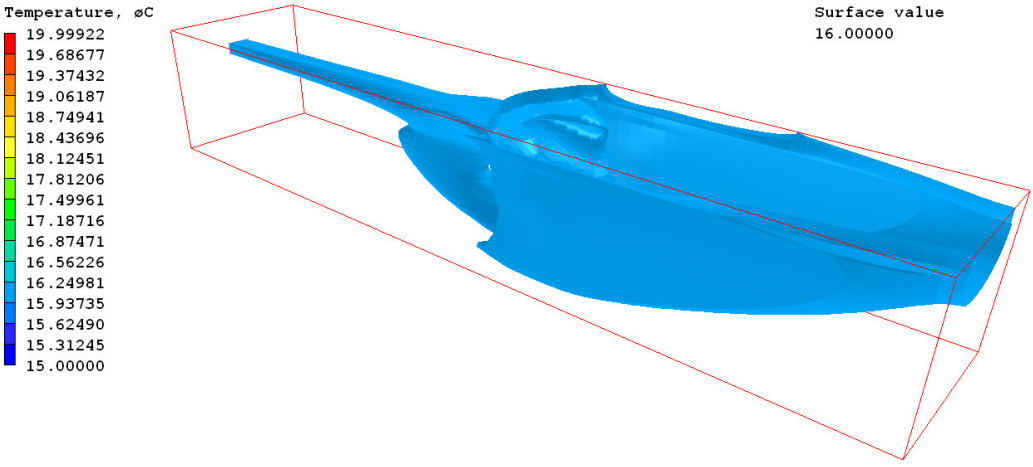

Figure 9 Temperature Iso-Surface of 16 ^{o}C for Case 3.

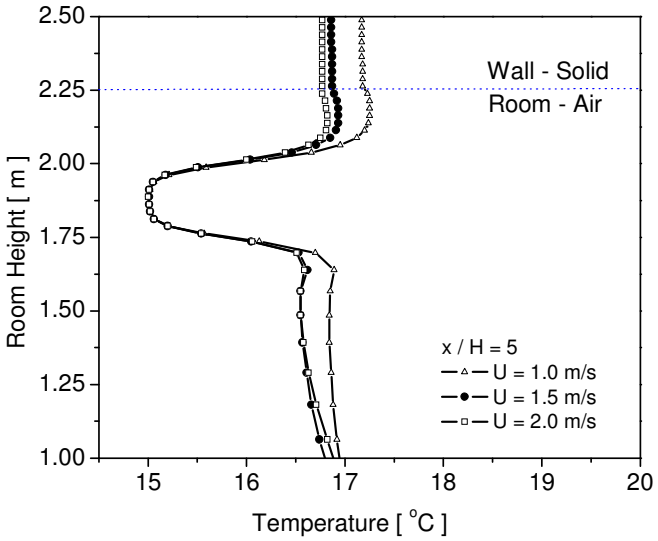

Figure 10 Temperature distribution at central line M1-M2.

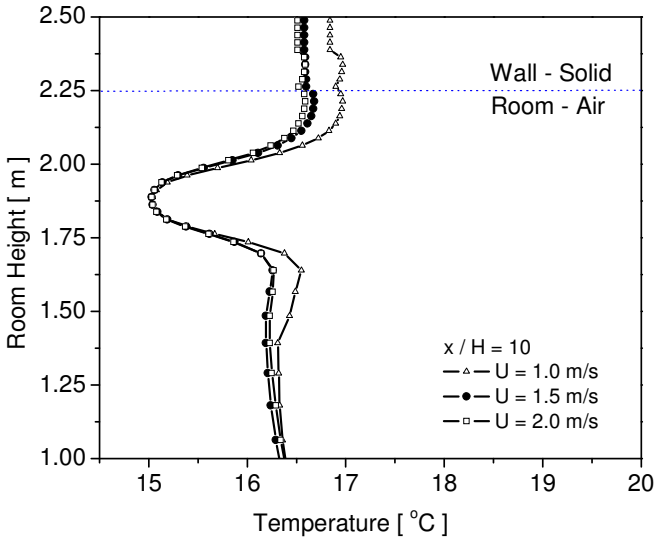

Figure 11 Temperature distribution at central line M3-M4.

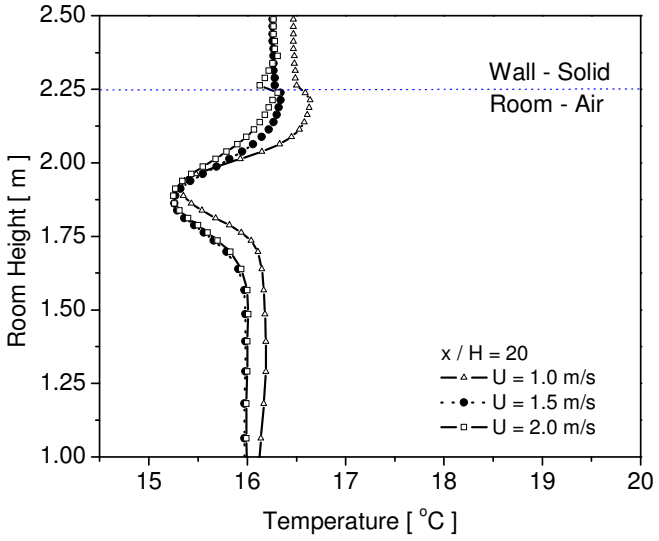

Figure 12 Temperature distribution at central line M5-M6.